ELSEVIER

Polymer 41 (2000) 8849–8855

polymer

www.elsevier.nl/locate/polymer

Simulation of thickening growth in polymer crystallisation

K.L. Anderson, G. Goldbeck-Wood*

Department of Materials Science and Metallurgy, University of Cambridge, Pembroke St., Cambridge CB2 3QZ, UK

Received 8 October 1999; received in revised form 11 February 2000; accepted 19 February 2000

Abstract

The scope of this work is to investigate polymer crystallisation involving thickening growth by means of a kinetic Monte Carlo simulation. The simulation combines the lateral growth mechanism of the Sadler/Gilmer model with Hikosaka's 'chain sliding diffusion' mechanism for thickening growth. As a result of this coupling of lateral and thickening growth, we obtain wedge-shaped crystals if the sliding friction is not too high ('mobile regime') and lamellar crystals for high friction. In the mobile regime the thickening rate increases with undercooling. Thickening also increases the lateral growth rate, especially at low undercooling, since it lowers the entropic and enthalpic barriers. As a result, the activation energy of both processes takes a similar value, in agreement with experiment. For high friction, the thickening rate increases with temperature up to a maximum close to the melting point, in agreement with the observations of thickening of lamellar polymer crystals. This simple model hence captures the essence of lateral and thickening growth behaviour in polymer crystallisation.

Keywords: Polymer crystallisation; Thickening growth; Sadler/Gilmer model

1. Introduction

It is well established that a wide range of semicrystalline polymers form ordered, chain-folded, lamellar crystals with a thickness of the order of 100 Å [1]. The thickness is a constant at a particular crystallisation temperature, or undercooling. In materials which crystallise below the α_c relaxation temperature [2], the chains are essentially locked into the crystal in the way in which they are first incorporated. In the case of crystallisation above $T_{\alpha c}$, as is the case in polyethylene, some thickening takes place following the initial attachment. Nevertheless, the crystal morphology remains lamellar and the thickness limited by folds and chain-ends.

In stark contrast to this 'normal' case is the formation of extended chain type, disordered crystals arising from crystallisation in so-called mobile phases which allow considerable longitudinal movement of the chains. A well-known example is that of the hexagonal phase of polyethylene, which under high hydrostatic pressure, gives rise to wedge-shaped single crystals [3]. This morphology arises from lateral 'chain-folded' type growth being accompanied by a continuous thickening growth immediately behind the growth front.

An understanding of thickening growth is of significance in many ways. It is a mode of growth found in several important polymers apart from polyethylene at high pressure [3]: e.g. poly(tetrafluoroethylene), poly(*trans*-1,4-butadiene) and vinylidene fluoride/trifluoroethylene copolymers [4]. In the latter case the growth of extended chain crystals is related to its piezoelectric properties. In the case of polyethylene thickening growth and the mobile phase have led to new perspectives on the mode of crystallisation [5], which have recently been utilised to produce perfectly sintered ultrahigh molecular weight material free from the usual grain texture [6].

The aim of this work is to understand more about the thickening growth process, and the way in which lateral and thickening growth influence each other. To this end we have carried out computer simulations based on an extended Sadler/Gilmer model of polymer crystallisation [7,8], as first outlined by one of us [9]. Before reporting on the results of the simulations, the pertinent experimental and theoretical background information will be summarised.

2. Background

2.1. Experimental evidence

Here we summarise the main experimental facts against which our simulations are to be tested:

* Corresponding author. Fax: + 44-1223-334567.
E-mail address: gg212@cam.ac.uk (G. Goldbeck-Wood).

0032-3861/00/$ - see front matter
PII: S0032-3861(00)00228-7

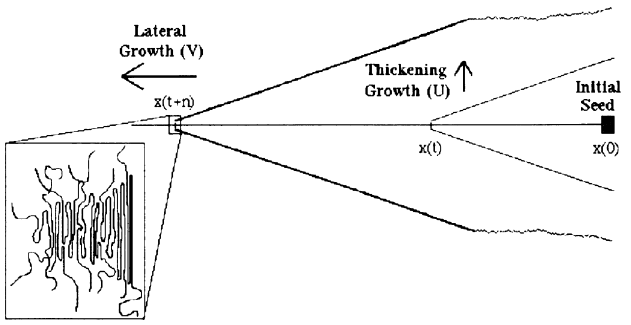

Fig. 1. Schematic edge-on view of thickening growth crystallisation, showing the thickening growth rate U and the lateral growth rate V.

(i) In the mobile phase, crystals grow both laterally and in the thickness direction leading to a wedge shape with an approximately linear gradient (Fig. 1).
(ii) The lateral growth in the mobile phase is much faster than in the ordered crystal phase, and can be observed already for a very small degree of undercooling [3].
(iii) In the mobile phase, the thickening growth rate increases with undercooling.
(iv) In the mobile phase of polyethylene both lateral and thickening growth rate measured in a *small* range of undercoolings can be expressed in the form [10]:

$$R = R_0\, exp(A/\Delta T) \tag{1}$$

where $\Delta T = T_m^0 - T_c$ is the undercooling below the crystallisation temperature, and the front factor R_0 is equal to 1000 nm s^{-1} for the lateral growth rate and 100 nm s^{-1} for the thickening rate, and the 'activation energy' A is 23 K for lateral and 20 K for thickening. It is not yet known whether such a relationship holds over a larger range of undercoolings.
(v) The taper angle ϕ decreases with undercooling following the above, as well as measurements shown earlier [11] which also indicate that the slope of $\phi(\Delta T)$ decreases with undercooling.
(vi) The rate of thickening of lamellar crystals in the ordered phase increases with temperature [3,12].

The issues arising from these observations are why thickening growth in the mobile phase increases with undercooling while it decreases with undercooling for thickening in the ordered crystal phase, and whether the similarity in the activation energy is due to a coupling of the lateral and thickening growth, i.e. is the thickening growth limited by material coming in laterally, or is the thickening the rate limiting factor, and why?

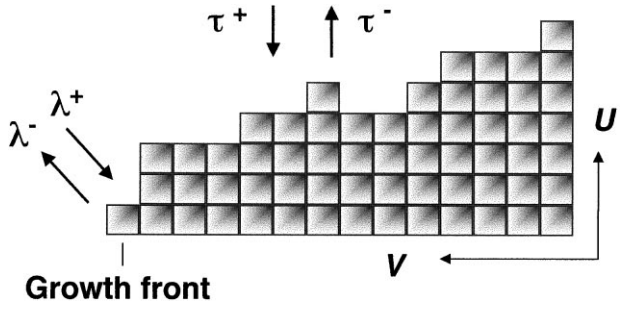

Fig. 2. Schematic representation of the thickening growth model showing the transition rate constants for additions and removals of the chain segments shown as blocks.

3. Theory

The main theoretical study of thickening growth is by Hikosaka [13,14]. His approach is based on the nucleation theory for polymers by Frank and Tosi [15]. The crucial feature of the Frank and Tosi theory in this context is that it allows the stem length of the nucleus to vary. Hikosaka proposed that material for thickening growth could become available via a mechanism of 'sliding diffusion' of polymer chains through the crystal. His model features a corresponding transport term in addition to the usual WLF term.

The activation energy for sliding diffusion, E_e, is given by Hikosaka as:

$$E_e = \kappa \ell^{\nu} \tag{2}$$

where κ and ν are parameters which represent the frictional behaviour of the chain sliding within the crystal, and ℓ is the stem length. As a result of this additional term, the free energy barrier for nucleation becomes a function of both the stem length ℓ and the number of lateral growth layers n. In order to allow for a closed solution Hikosaka assumes the thickness ℓ to be a function of n in the following way

$$\ell = Cn^{\xi} \tag{3}$$

where C is a constant. The power ξ is called the 'path parameter', and describes the type of crystal that is growing. For low values (closer to 0) of ξ the crystal aspect ratio is similar to that of a lamella, and for higher values (closer to 1) the growing crystal resembles extended chain crystals.

The analytical treatment by Hikosaka has been fitted successfully to the behaviour of polyethylene [13,14]. However, it requires a number of assumptions, and does not allow the actual wedge shape, nor rates to be computed, nor is it possible to study the interdependence of thickening and lateral growth in detail, since their dependence is already to some extent fixed by means of the path parameter.

4. The model

Our model, shown schematically in Fig. 2, represents a polymer single crystal by a two-dimensional slice cut out of a crystal perpendicular to the growth front. The crystal model is made up out of blocks which represent segments of the polymer chain. Each column of blocks is called a stem. The stem length ℓ is given in terms of the dimensionless number of blocks. The blocks interact with their nearest neighbours only, by means of interaction energies ϵ_1 and ϵ_2

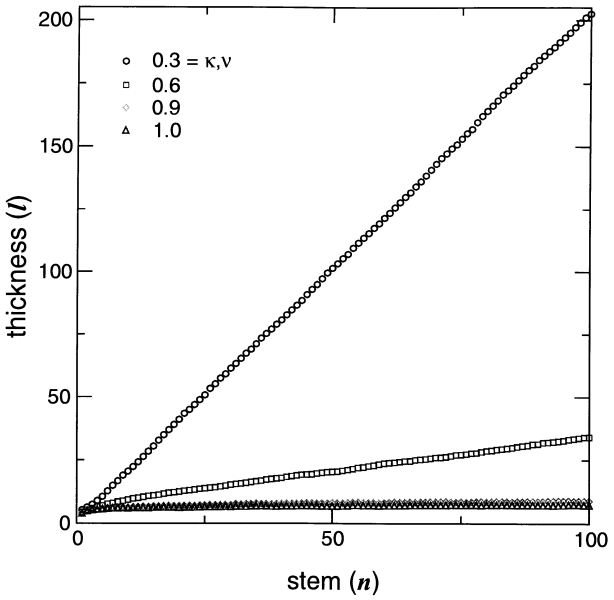

Fig. 3. Crystal shapes for a range of friction constants $\kappa = \nu$ at $T_c/T_m^0 = 0.91$. The crystal outlines are averaged of 100 runs, and their respective growth fronts have been aligned for comparison.

along and between stems, respectively. A fold energy ϵ_f is assigned to the first unit in a stem.

Growth starts from a seed crystal and proceeds by a Monte Carlo algorithm deciding about solid-on-solid additions and removals of blocks. Since it is envisaged that two processes contribute to the growth, a chain-folded lateral growth mode and a thickening growth by chain sliding diffusion, there are two separate Monte Carlo processes which are executed in each time step.

For the lateral growth, the model is identical to the Monte Carlo version of the Sadler/Gilmer row model of polymer crystallisation [9]: in each time step, a block can either be added onto or in front of the foremost stem, or the last added block removed. These rules of attachment mimic the chain-folded crystallisation. The rate constants for the different events are as follows. For all additions:

$$\lambda^+ = \exp\left(-\frac{\epsilon_1 + \epsilon_2}{kT_m^0}\right), \tag{4}$$

for removal from a niche site:

$$\lambda_n^- = \exp\left(-\frac{\epsilon_1 + \epsilon_2}{kT_c}\right), \tag{5}$$

for removal from an overshoot site:

$$\lambda_o^- = \exp\left(-\frac{\epsilon_1}{kT_c}\right), \tag{6}$$

and for removal from a fold site:

$$\lambda_f^- = \exp\left(-\frac{\epsilon_1 + \epsilon_2 - \epsilon_f}{kT_c}\right). \tag{7}$$

In the above, T_m^0 denotes the equilibrium melting point of the material, and T_c the (isothermal) crystallisation temperature.

It was shown in earlier simulations of chain-folded crystallisation that this two-dimensional model of lamellar crystallisation captures the essential features [7,8] and can even be fitted to experimental data [9].

In the Sadler/Gilmer model any thickening behind the first growth layer is forbidden in order to account for the effects of high lattice forces and chain-folds, ends, and entanglements on the top and bottom surfaces. In the thickening growth mode, however, the addition of blocks to the 'fold' surface is permitted. To this end, a second 'sliding diffusion' process is implemented on the top surface in parallel to the lateral growth process. First, the transport of polymer by means of chain sliding is modelled by the Arrhenius term

$$P = \exp\left(-\frac{E_e}{kT_c}\right) \tag{8}$$

with an activation energy E_e as given by Eq. (2). We use a constant value of the activation energy for stem lengths exceeding a particular cutoff thickness value ℓ_{cutoff}, i.e.

$$E_e = \kappa \ell_{cutoff}^{\nu} \quad \text{for } \ell > \ell_{cutoff}. \tag{9}$$

The rationale for this restriction is that there are point defects in the disordered crystal and hence slack in the chain which limits the length contributing to the sliding friction.

Once this transport barrier is overcome, crystallisation is simulated by a kinetic Monte Carlo algorithm with the following rate constants

$$\tau^+ = 1 \tag{10}$$

for all additions, and

$$\tau^- = \exp\left(-\frac{(\epsilon_1 + \epsilon_2)(T_m^0 - T_c) + \epsilon_2(N-1)}{kT_c}\right) \tag{11}$$

for removal from a site with N lateral neighbours.

In general the thickening process was made to work on all stems except the first one since the lateral addition process, i.e. chain-folded crystallisation is active at the growth front. As in previous work [7–9], the simulations are carried out on only one surface, with the assumption of symmetry for the opposite (bottom) surface.

In the following we present results on the shapes generated, the lateral and thickening growth rates for the cases of high- and low-mobility, and an analysis in terms of the path parameter introduced by Hikosaka.

5. Results and discussion

Simulations were carried out using the following values of the interaction parameters unless otherwise stated: $\epsilon_1 = \epsilon_2 = \epsilon_f = 3kT_m^0$. Previous simulations [7,9] have shown that

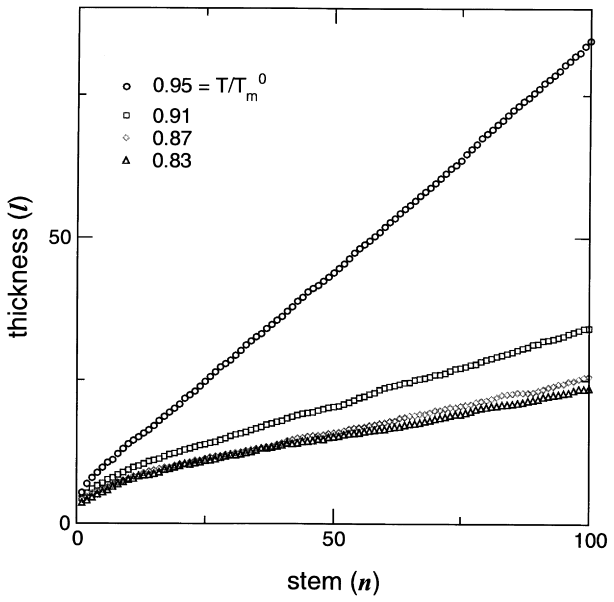

Fig. 4. Crystal shapes for $\kappa = \nu = 0.5$ and different dimensionless crystallisation temperatures $T = T_c/T_m^0$.

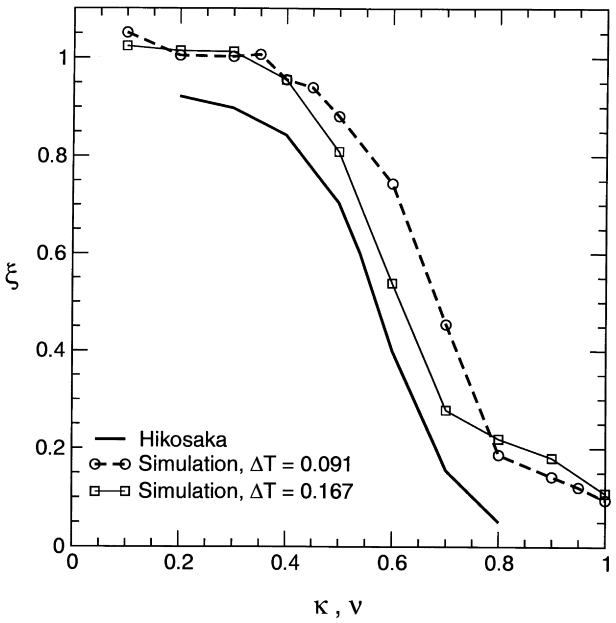

Fig. 6. Path parameter for different undercoolings. The result from Hikosaka [13] is shown for comparison.

this value reflects typical flexible polymer crystallisation behaviour.

The sliding energy parameter κ will be given in multiples of $k_B T_m^0$, and the exponent ν is a dimensionless number. We investigated the effects of both parameters κ and ν ranging from 0.1 (low friction) to 10 (high friction), mostly for the case $\kappa = \nu$, as done by Hikosaka, but also varying just one and keeping the other constant. The cutoff thickness ℓ_{cutoff} was in general set to 10. All the results reported are averages over between 100 and 1000 runs starting from a seed crystal of height and length 10 and were grown to a lateral size of 200 stems.

The following results hence explore the typical crystallisation behaviour involving thickening growth, and are not aimed at quantitative comparisons with certain polymers.

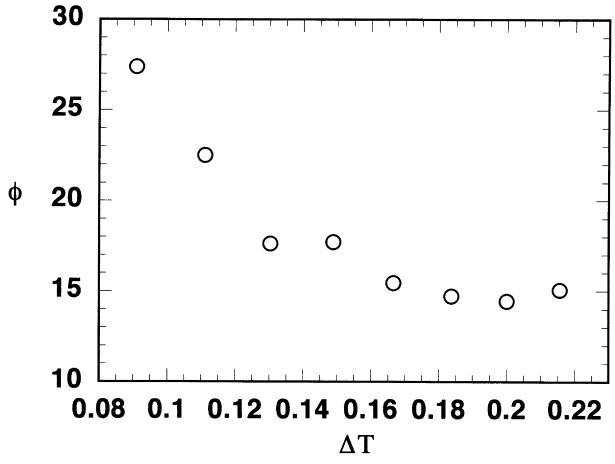

Fig. 5. Taper angle ϕ as a function of undercooling for $\kappa = \nu = 0.6$.

Nevertheless, we can draw qualitative comparisons with the experimental observations outlined above.

5.1. Crystal shapes and thickness

The two-dimensional crystal slices generated by the kinetic Monte Carlo simulation can be viewed as edge-on shapes of crystals. The resultant shape depends strongly on the κ and ν values chosen, as can be seen in Fig. 3. For κ and ν values close to 1 the crystal shape resembles that of a lamellar crystal, whereas values nearer to zero lead to considerable thickening and hence a wedge-shaped crystal, in qualitative agreement with the experimental observation (i).

In addition to the 'friction' the shape of the crystal is affected by the undercooling. Fig. 4 shows a number of crystals grown at different undercoolings, but all with the same friction constants $\kappa = \nu = 0.5$. As expected from such a low value, we see considerable thickening. The taper angle ϕ (Fig. 5) is largest at small undercooling, and then flattens off to an approximately constant value. This finding is in line with the experimental observation (v) above.

In order to analyse the shape of the crystal and the transition from the lamellar to the extended chain morphology we have fitted the shape of the crystal according to Hikosaka path parameter Eq. (3). However, in the presence of lateral growth ξ is a measure of the shape of the crystal rather than of the aspect ratio of a rectangular nucleus. It can be evaluated by taking a linear regression of $\log \ell$ versus $\log n$, and the result for different undercoolings is shown in Fig. 6. Similar to Hikosaka's analysis [13,14], we observe a pronounced transition from the chain-extending type growth (ξ close to one) to the lamellar type (ξ close to zero). The

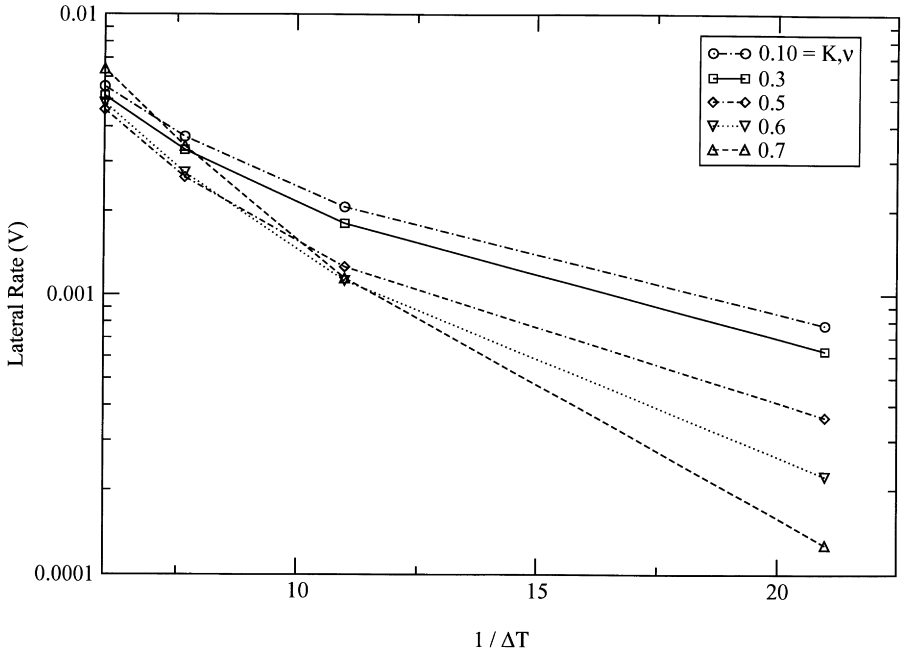

Fig. 7. Lateral growth rates as a function of the reciprocal dimensionless undercooling for different friction constants $\kappa = \nu$.

transition is slightly shifted and less sharp at higher undercoolings.

5.2. Growth rates

As noted in Section 2, both the lateral and the thickening growth rates are expected to follow a relation of the form of Eq. (1) where G_0 and A are constants at least within certain ranges of undercooling. Fig. 7 shows that the lateral growth rates can indeed be represented in this way. We note the increase in the slope with increasing undercooling, which is sometimes interpreted as a transition to Regime III [16]. Of particular interest here is the pronounced effect which the sliding coefficients κ, ν have on the lateral growth rate at smaller undercooling: if thickening behind the growth front is made easier, the lateral growth rate increases. The reason for this increase lies in the lowering of the barriers to lateral growth which increase strongly with increasing stem length.

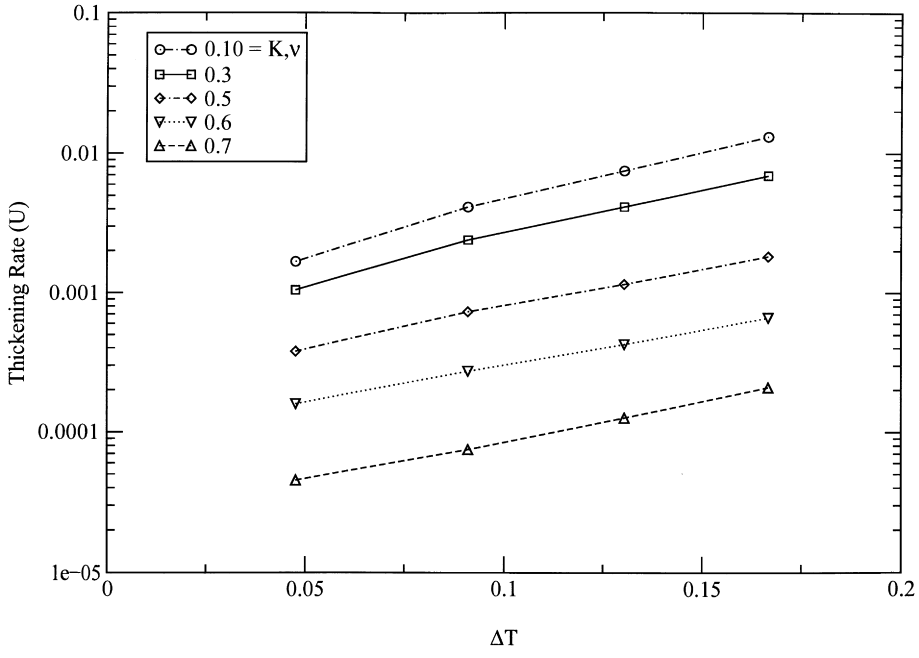

Fig. 8. Thickening growth rates as a function of dimensionless undercooling and temperature for different friction constants $\kappa = \nu$.

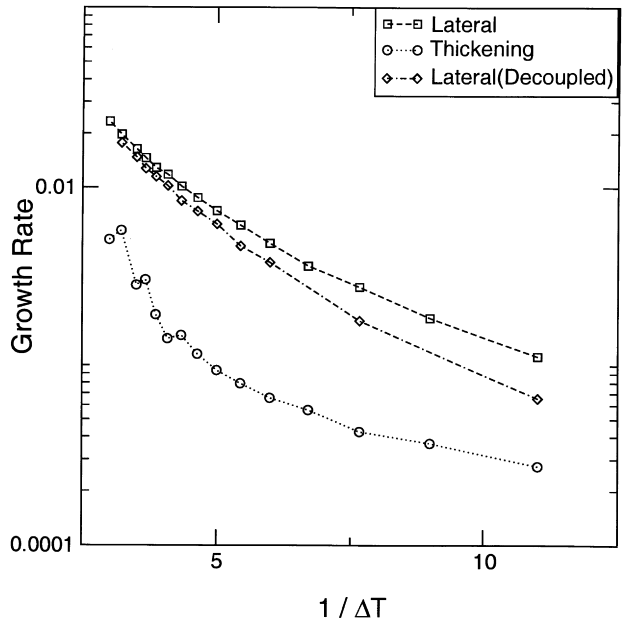

Fig. 9. Comparison of lateral and thickening growth rates for $\kappa = \nu = 0.6$. Also shown is the lateral growth rate if decoupled from thickening.

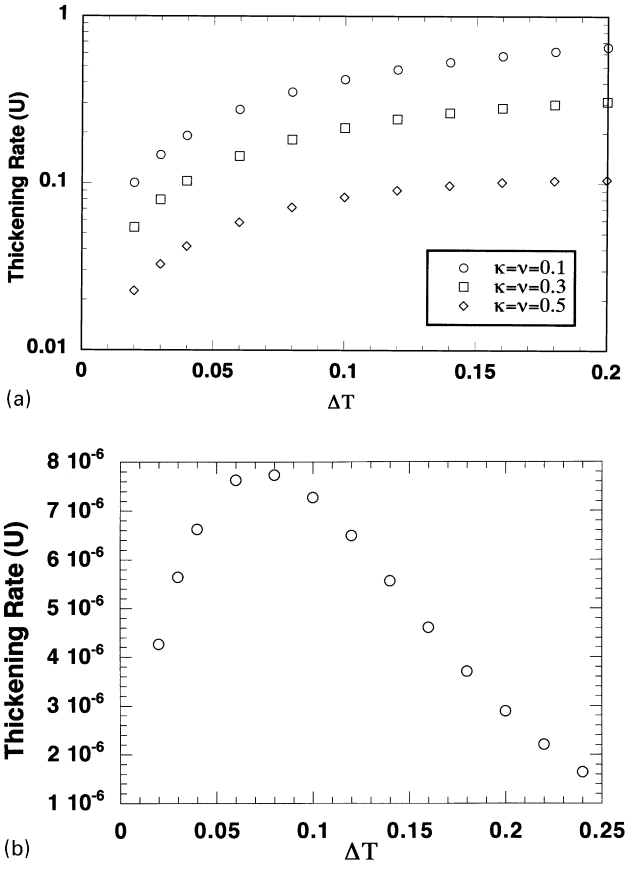

Fig. 10. Analytical results for the average thickening rate according to Eq. (12): (a) for small $\kappa = \nu$ (taking $\ell = \ell_{\text{cutoff}} = 20$ for $\kappa = \nu = 0.1$ and 0.3, and $\ell = 7$ for $\kappa = \nu = 0.5$); and (b) for large $\kappa(\kappa = 10)$ and $\nu = 0$.

In pure lateral growth, an entropic barrier arises from the fact that there are many additions which lead to a tapered edge with a stem thickness below the minimum stable thickness. The growth front can only proceed by remelting of those stems and a 'squaring off' of the crystal [7]. In addition, there is an energy barrier for 'overshoot' blocks, i.e. ones protruding above the neighbouring stems [17,18]. Both barriers will be lowered as a result of thickening. A similar phenomenon was found for growth onto a thicker crystal surface or substrate [8,17]: the growth rate is increased with respect to the steady state. However, in the latter case the increase is only transient: as the thickness decays towards the steady state, so does the growth rate. In the thickening growth case however, an increased steady state rate is obtained. The fact that the thickening has very little effect at large undercooling is due to the small critical size so that most attachments can be incorporated into the crystal regardless of any thickening.

The thickening growth rates are shown in Fig. 8. As expected, they increase with decreasing κ, ν values and increase with undercooling in agreement with observation (iii) above. In fact, a logarithmic plot of the lateral and thickening rates versus ΔT (Fig. 9) shows that the model can reproduce observation (iv): over a range of undercoolings both rates can be fitted by Eq. (1) with a similar exponent A, and lateral growth about ten times larger than thickening growth.

In order to analyse the coupling of the lateral and thickening rates further, the basic algorithm described above was modified so that thickening growth would only start five layers behind the growth front, thereby decoupling the two processes. Fig. 9 shows that the decoupled lateral growth rate decreases much more strongly with undercooling. For larger undercoolings, the coupled and uncoupled rates converge, due to the kinetic driving force. This result proves that the lateral growth process is, at low undercooling at least, a 'slave' to the thickening taking place behind the growth face.

The point which has not been addressed yet, is number (vi) of experimental evidence: the thickening in the lamellar case was found to increase with temperature. All the results presented so far, even for values of κ, ν which yield lamellar morphologies show the opposite behaviour. A simple analysis of the thickening in the model, however, reveals the wider picture. The net thickening rate is the result of two independent processes: transport through sliding; and crystal growth in the thickness direction. Hence, with Eqs. (8–11), and neglecting the surface interaction term, the average thickening rate is:

$$\bar{U} = \left[1 - \exp\left(-\frac{\Delta H \Delta T}{\mathrm{k} T_\mathrm{c} T_\mathrm{m}^0}\right)\right] \exp\left(-\frac{E_\mathrm{e}}{\mathrm{k} T_\mathrm{c}}\right) \tag{12}$$

where $\Delta H = \epsilon_1 + \epsilon_2$ is the heat of fusion of the model crystal. Clearly, this function is zero at both 0 K and T_m^0 with a maximum in between. If for simplicity we assume the sliding friction to be constant with thickness ($\nu = 0$), the

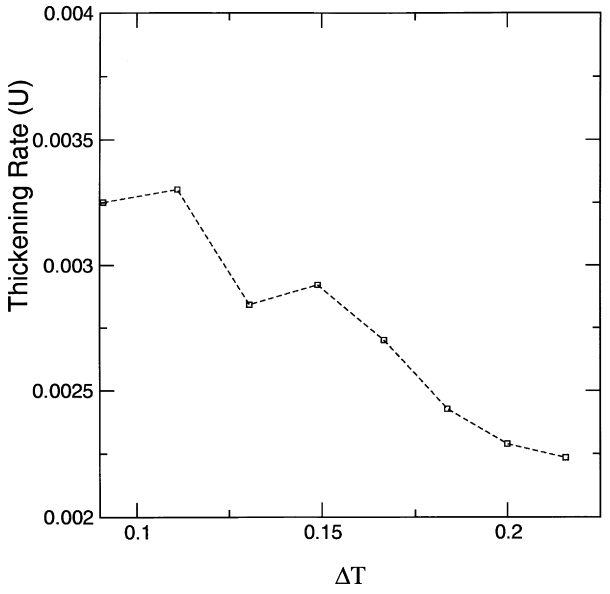

Fig. 11. Thickening rate from simulations with large $\kappa(\kappa = 10)$ and $\nu = 0$ showing the decrease with undercooling observed for lamellar thickening.

maximum can be obtained after differentiation with respect to temperature:

$$T_{\max} = T_{\mathrm{m}}^{0}\left[1 + \frac{\mathrm{k}T_{\mathrm{m}}^{0}}{\Delta H}\ln\left(\frac{E_{\mathrm{e}} + \Delta H}{E_{\mathrm{e}}}\right)\right] \tag{13}$$

This equation shows that the maximum temperature decreases with decreasing sliding friction. It becomes clear that, in the range of small κ, ν the thickening rate increases with undercooling in the range observed, as confirmed by Fig. 10a. The increase is linear as would be expected from the first term of Eq. (12). However, we emphasise that Eq. (12) is only an approximation, and the thickening rate observed from the simulation, in which lateral and thickening growth are coupled, is exponential (Fig. 8).

If the sliding friction is substantially larger the thermally activated process dominates and the maximum shifts closer to the melting point (Fig. 10b). In this case thickening would be observed to increase with temperature. If we replaced the Arrhenius term (8) for the sliding by a WLF term with respect to $T_{\alpha\mathrm{c}}$, as would be more appropriate, $T_{\max}$ would shift to an even higher value. Fig. 11 finally demonstrates that the lamellar thickening of the ordered phase is also reproduced by our simulations. There are considerable fluctuations since the absolute values of thickening are very small at such high values of friction.

6. Conclusions

The thickening growth simulations have reproduced successfully the range of experimentally observed morphologies (from lamella to wedge shape) and growth behaviour (from chain-folded to chain-extending crystallisation).

Thickening growth leads to a reduction in the growth barrier for lateral growth. As a result the lateral growth rate is increased strongly at small undercooling, and the lateral and thickening growth rates have an exponential dependency on undercooling with a similar ‘activation energy’, in agreement with experiment. The simulations have shown that thickening rather than lateral growth is the dominant factor.

Both the thickening growth observed in the mobile phase as well as that observed in lamellar crystals above T_{ac} can be explained within one model which takes both the thermally activated chain motion and the undercooling driven crystallisation into account. As a result the thickening rate has a maximum at a temperature which depends on the sliding friction. If the chain motion is relatively easy, the undercooling term dominates and the thickening rate increases with undercooling for all of the accessible temperature range, whereas for low mobility the opposite is the case. The model hence provides a simple but coherent picture of thickening growth in polymer crystallisation.

Acknowledgements

We would like to thank the Cambridge HPCF for providing access to their PC cluster, and Dr Peter Barham for a probing question at the ACS symposium which led us to investigate the thickening behaviour in the lamellar case.

References

[1] Keller A, Goldbeck-Wood G. In: Aggarwal SL, Russo S, editors. Comprehensive polymer science, Oxford: Pergamon Press, 1996. p. 241–305 (Second Suppl.).
[2] Hu W-G, Schmidt-Rohr K. Acta Polym 1999;50:271–85.
[3] Hikosaka M, Amano K, Rastogi S, Keller A. Macromolecules 1997;30:2067–74.
[4] Hattori T, Watanabe T, Akama S, Hikosaka M, Ohigashi H. Polymer 1997;38:3505–11.
[5] Keller A, Goldbeck-Wood G, Hikosaka M. Faraday Discuss. 1993;95:109–28.
[6] Rastogi S, Kurelec L, Lemstra PJ. Macromolecules 1998;31:5022–31.
[7] Sadler DM, Gilmer GH. Phys Rev B 1988;38:5684–93.
[8] Goldbeck-Wood G. Simulation of polymer crystallisation. In: Dosière M, editor. Crystallisation of polymers, NATO ASI Series, Ser. C, vol. 405. Dordrecht: Kluwer, 1993. p. 249–55.
[9] Goldbeck-Wood G. Macromol Symp 1994;81:221–34.
[10] Hikosaka M, Okada H, Toda A, Rastogi S, Keller A. J Chem Soc Faraday Trans 1995;91(16):2573–9.
[11] Hikosaka M, Amano K, Rastogi S, Keller A. Lamellar thickening growth of an isolated extended chain single crystal of PE. In: Dosière M, editor. Crystallisation of polymers, NATO ASI Series, Ser. C, vol. 405. Dordrecht: Kluwer, 1993. p. 331–6.
[12] Peterlin A. Macromol Chem 1964;74:107.
[13] Hikosaka M. Polymer 1987;28:1257–64.
[14] Hikosaka M. Polymer 1990;31:458–68.
[15] Frank FC, Tosi M. Proc R Soc London 1961;A263:323–39.
[16] Hoffman JD. Polymer 1983;24:3–26.
[17] Doye JPK, Frenkel D. J Chem Phys 1999;110(5):2692–2702 .
[18] Doye JPK, Frenkel D. J Chem Phys 1999;110(14):7073–86.